FEATURES OF THE NORTHERN SMOOTH PLAINS OF MERCURY REVEALED BY DETRENDED MLA TOPOGRAPHY: COMPARISON WITH THE MOON. M. A. Kreslavsky[1,2], J. W. Head[3], G. A. Neumann[4], M. T. Zuber[5], D. E. Smith[5], [1]Earth and Planetary Sciences, University of California, Santa Cruz, CA, 95064, USA, mkreslav@ucsc.edu; [2]MExLab, Moscow State University of Geodesy and Cartography (MIIGAiK), Moscow, Russia; [3]Earth, Environmental and Planetary Sciences, Brown University, Providence, RI, 02912, USA; [4]Solar System Exploration Division, NASA Goddard Space Flight Center, Greenbelt, MD, USA; [5]Earth, Atmospheric and Planetary Sciences, MIT, Cambridge, MA, USA.

Introduction: Despite great advances in computer data processing, visual inspection remains a basic analysis tool in geomorphology. Laser altimeter data are, in a sense, too precise for visual perception. For example, the internal ranging precision of the Mercury Laser Altimeter (MLA) [1] onboard the MErcury, Surface, Space, ENvironment, GEochemistry, and Ranging (MESSENGER) mission is about 12 cm, and the topographic amplitudes on Mercury exceed ~5 km, which gives an impressive dynamic range; without special effort this accuracy of the data could remain unused. To fully actualize the great potential of laser altimeter data in sensing low-amplitude gently sloping topographic features we apply a special detrending algorithm, which enables visualization of subtle topographic features in smooth terrains. The same detrending algorithm has been successfully applied to martian [2] and lunar [3] topography.

Detrending procedure: As source data for the detrended topographic map of Mercury (Fig. 1), we use a preliminary version of the MLA Gridded Data Records from the PDS. Because of MESSENGER orbit constraints, MLA data coverage is sufficient for detailed topographic mapping only in the northern polar area, therefore we used the interpolated gridded topographic map in polar azimuthal stereographic projection at 500 m per pixel sampling. Northward from ~ 60º latitude the majority of pixels in this source map are obtained from actual MLA ranging measurements rather than by interpolation.

The detrended topography at each pixel was calculated as a difference between the actual elevation at this pixel and the median elevation of all pixels within a circular window centered at this pixel. The window size defines the spatial scale of the features that are considered as a global trend and thus are subject to removal. We used a window radius of 10 pixels, which is equivalent to 10 km in diameter. The reduced resolution version of the resulting map is shown in Fig. 1.

The filtering algorithm used is similar to high-pass linear filters, however, we use the median in a sliding window to calculate the trend surface, while the linear filters use the weighted arithmetic mean. Any reasonable detrending algorithm, including both our median-based and the traditional linear filters, filters out topographic features much larger than the window, preserves topographic features much smaller than the window, and distorts features comparable to the window in size. Our algorithm produces less distortion than linear filters, which makes the results of the median-based detrending much better for visual perception than the results of a linear high-pass filter. This was the principal reason for our choice of the median-based detrending.

The actual accuracy of MLA topographic measurements is lower than the internal ranging precision due to inaccuracies in MESSENGER orbit and attitude knowledge [1]. Detrending reveals spurious features appearing as sub-parallel lines (Fig. 1); they are abundant at lower latitudes, where the data density is lower.

Any detrending algorithm significantly distorts features comparable to the window size. Due to the nonlinear nature of the median-based detrending procedure, distortions of window-scale features are more complicated, than for a linear high-pass filter. Typical heavily cratered terrains on Mercury, including vast intercrater plains, have many craters and other topographic features in the "harmful" 5- 20 km size range. As a result, the detrended topography technique is much more useful in the regionally flatter smooth plains [4-6]. Fortunately, a significant part of the mapped northern polar area of Mercury (Fig. 1) is occupied by smooth plains of Borealis Planitia.

Topographic texture of smooth plains: Smooth plains in the map (Fig. 1) are covered with a dense quite isotropic network of bright (positive detrended topography) lineaments that represent wrinkle ridges and smooth convex slope breaks. Almost all these lineaments are distinguishable in low-sun images taken under favorable illumination geometry. However, the detrended topography map is better for their detection: it is free of biases related to sun elevation and azimuth.

Many bright lineaments in Borealis Planitia (Fig. 1) are circles; some of them are concentric; many such circles are slope breaks outlining smooth shallow circular depressions, "ghost craters" [4,6,7]. All these circles obviously outline buried craters and double-ring basins that existed before the final emplacement of smooth-plains-forming lavas. On the Moon only a few features of this kind are known [3]. Their abundance on Mercury may be related to the lack of terrain resetting by large basin formation in the northern plains, and by the very

high resurfacing rates of volcanic plains emplacement [4,6].

On the Moon, the detrended topography maps [3] readily reveal smooth low-topography volcanic constructs (mare domes and small shields) amid mare-forming volcanic plains. No similar features are observed in Borealis Planitia [4] on Mercury, which is another aspect of the difference between the volcanic styles of plain-forming volcanism on the Moon [9] and Mercury [4-6].

References: [1] J. Cavanaugh et al. (2007) *Space Sci. Rev. 131,* 451. [2] M. Kreslavsky & J. Head (2001) *JGR 107*, 5121, DOI: 10.1029/2001JE001831. [3] M. Kreslavsky et al. (2016) *LPSC 47*, #1331. [4] J. Head et al. (2011) *Science* 333, 1853. [5] B. Denevi et al. (2013) *JGR 118,* 891. [6] L. Ostrach et al. (2015) *Icarus* 250, 602. [7] C. Klimczak et al. (2012) *JGR 117*, E00L03. [8] J. Head & A. Gifford (1980) *Moon* 22, 235. [9] J. Head and L. Wilson (2016) *LPSC 47*, #1189.

Acknowledgements: We acknowledge support from the NASA SSERVI grant to Brown University. All technical work on data analysis was carried out by MAK at MIIGAiK under Russian Science Foundation support, project 14-22-00197.

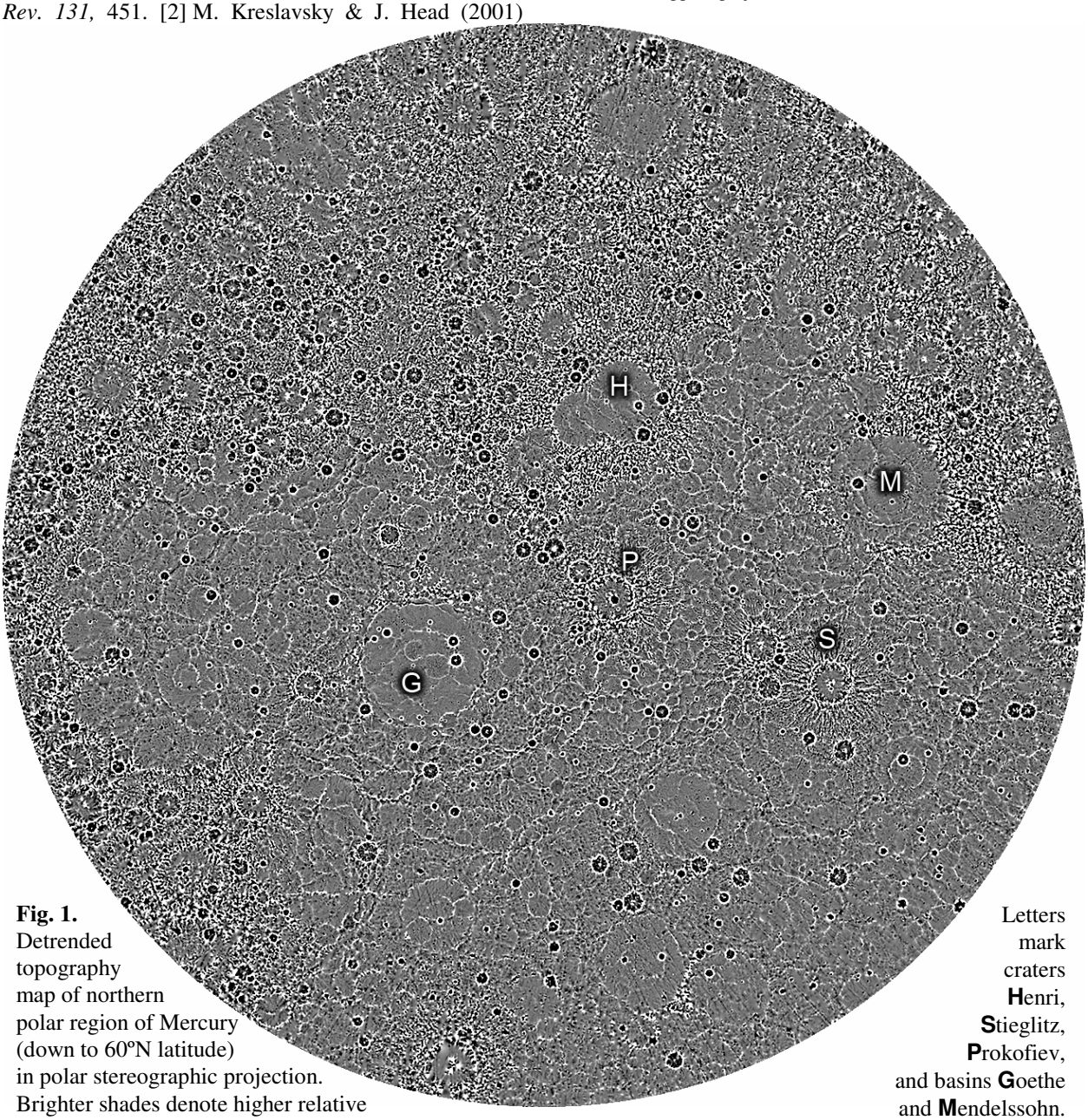

Fig. 1. Detrended topography map of northern polar region of Mercury (down to 60ºN latitude) in polar stereographic projection. Brighter shades denote higher relative elevation. Letters mark craters **H**enri, **S**tieglitz, **P**rokofiev, and basins **G**oethe and **M**endelssohn.